Microjet Cooling Devices for Thermal Management of Electronics

Dan S. Kercher, Jeong-Bong Lee, Oliver Brand, Mark G. Allen, *Member, IEEE,* and Ari Glezer

***Abstract*—This research is an effort to demonstrate the applicability of miniaturized synthetic jet (microjet) technology to the area of thermal management of microelectronic devices. Synthetic jets are jets which are formed from entrainment and expulsion of the fluid in which they are embedded. Design issues of microjet cooling devices are discussed along with characterization of excitation elements and the turbulent synthetic jets produced thereby. Geometrical parameters of the microjet cooling devices were empirically optimized with regards to cooling performance. The cooling performance of the optimized microjets was compared with previous theoretical and empirical studies of conventional jet impingement. The cooling performance of the microjet devices has been investigated in an open environment as well as in a vented and closed case environment. In such experiments, the synthetic jet impinges normal to the surface of a packaged thermal test die, comprising a heater and a diode-based temperature sensor. This test assembly allows simultaneous heat generation and temperature sensing of the package, thereby enabling assessment of the performance of the synthetic jet. Using microjet cooling devices, a thermal resistance of 30.1 °C/W has been achieved (when unforced cooling is used, thermal resistance is 59.6 °C/W) when the test chip is located at 15 mm spacing from the jet exit plane. In order to more directly compare and scale the cooling results, a preliminary study on heat transfer correlations of the microjet cooling device has been performed. Finally, a comparison of the performance of the microjet cooler with standard cooling fans is given.**

***Index Terms*—Closed case environment, conventional jet impingement, cooling fans, diode-based temperature sensor, electronics, entrainment, fluid, jet exit plane, microjet cooling device, open environment, thermal management.**

I. Introduction

HIGHER levels of integration of electronic circuits are common in both military and commercial electronic devices. Stringent thermal environments require increased thermal management of these devices. An example of these requirements is the cooling of a central processing unit (CPU) in an electronic system. A CPU cooling fan, in conjunction with a heat sink, provides the most common type of heat removal method for these high performance electronics devices [1]. Recently, jet impingement cooling of electronics has been investigated using pumps and convergent nozzles [2]–[4]; however, such approaches require a source of fluid and some means for pumping. Synthetic jets [5], [6] are jets which are formed from entrainment and expulsion of the fluid in which they are embedded. Such jets do not require a fluid source, eliminating the need for input piping and complex fluidic packaging.

In this work, the efficacy of synthetic microjet technology for electronic cooling has been investigated. This paper gives a brief overview of turbulent synthetic jet technology and describes design issues of the microjet cooling devices. Different driving elements, geometries, and configurations, and the resultant turbulent jets, are characterized and optimized. In order to more directly compare and scale the cooling results, a preliminary study on heat transfer correlations of the microjet cooling devices is presented. Finally, a comparison of the performance of the microjet cooler with standard cooling fans is given.

II. Microjet Cooling Device

A device for creating a synthetic jet consists of a cavity, bounded on one side by an orifice, and on the other side by a flexible membrane as shown in Fig. 1(a). When the flexible membrane is vibrated by a suitable driver, air is drawn into the cavity through the orifice [Fig. 1(b)] and ejected out of the cavity through the same orifice, forming a series of vortex rings which propagate away from the orifice, each under its own self-induced velocity [Fig. 1(c)]. A nominally round turbulent jet is synthesized as these vortex rings interact downstream. The distinctive characteristic of the synthetic jet is that it does not require a fluid source but is generated locally from the fluid adjacent to the surface of the orifice plate, thereby allowing momentum transfer into the surrounding fluid without net mass injection (i.e., zero-net-mass-flux) into the overall system [5].

The microjet cooling devices (Fig. 2) consist of a vibrating diaphragm, a diaphragm driver, and a housing with an orifice. In this work, the diaphragm consists of a circular latex membrane with a diameter of 25 mm and a thickness of 225 μm. The driver is electromagnetic and consists of a set of permanent magnets and a driving coil. Two cylindrical NdFeB permanent magnets, each with a diameter of 5 mm and a height of 6 mm, are affixed to opposite sides of the diaphragm at its center. The solenoidal coil has a diameter of 11 mm, a height of 10 mm, and a resistance of 22 Ω, and is held in position above the magnets by the machined aluminum housing. The latex membrane is stretched to the desired tension and clamped in place in the housing resulting in a specific diaphragm resonance frequency.

Manuscript received December 1, 2002; revised April 10, 2003. This work was supported in part by the U.S. Army Aviation and Missile Command (AMSAM), and the Microelectronics Research Center, Georgia Institute of Technology. This work was recommended for publication by Associate Editor S. Bhavani upon evaluation of the reviewers' comments.

D. S. Kercher, O. Brand, and M. G. Allen are with the School of Electrical and Computer Engineering, Georgia Institute of Technology, Atlanta, GA 30332-0269 USA (e-mail: mallen@ee.gatech.edu).

J.-B. Lee is with the School of Electrical and Computer Engineering, Georgia Institute of Technology, Atlanta, GA 30332-0269 USA, and also with the Department of Electrical Engineering, University of Texas at Dallas, Richardson, TX 70893-0688 USA.

A. Glezer is with the School of Mechanical Engineering, Georgia Institute of Technology, Atlanta, GA 30332-0269 USA.

Digital Object Identifier 10.1109/TCAPT.2003.815116

1521-3331/03$17.00 © 2003 IEEE

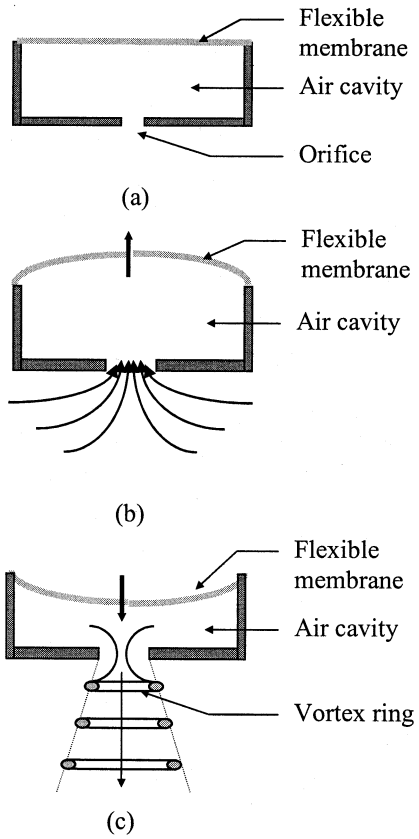

Fig. 1. Schematic diagrams of a turbulent synthetic jet device and generation of synthetic jets: (a) a turbulent synthetic jet device with its basic components: a driving element, a flexible membrane, an air cavity, and an orifice hole, (b) entrainment of air, and (c) vortex ring formation.

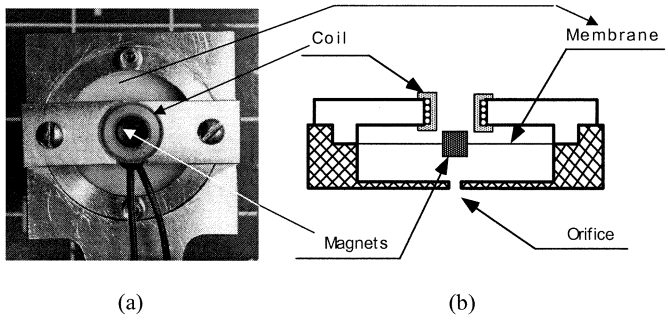

Fig. 2. (a) Photomicrograph of top view of the microjet cooling device and (b) a schematic diagram of the microjet cooling device.

An ac signal applied to the coil generates an alternating magnetic field, resulting in a periodic force acting on the magnets, and therefore on the membrane, inducing it to vibrate.

The desirable frequency response of the vibrating membrane is a large amplitude vibration at a specific frequency (i.e., a high quality factor of resonance). This is facilitated by the lumped mass of the magnets in the center of the tensioned diaphragm. Ultimately, the relatively high air damping in the microjet cooling application will limit the achievable quality factor.

Although the resonance frequency of the diaphragm is set by the tension, mass, and geometric parameters of the microjet cooling device, small changes in the resonant frequency could

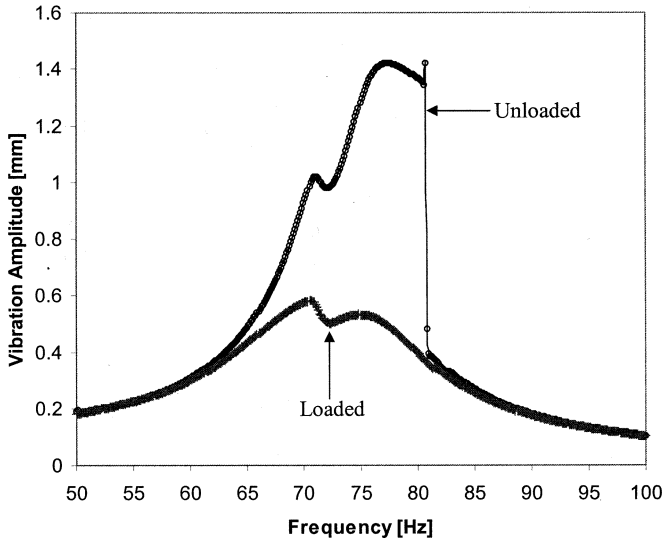

Fig. 3. Vibration amplitude, A, at the center of the latex membrane-based microjet cooling device as a function of the frequency for a driving voltage of $V_{ac} = 450$ MV rms; the vibration amplitude is shown for a loaded (with orifice plate) and an unloaded (without an orifice plate) membrane.

be induced by environmental factors. For example, temperature changes could cause changes in the diaphragm tension, with a resultant change in diaphragm resonant frequency. If the coil is driven at a fixed frequency, possible off-resonant operation due to these effects could result in nonoptimal performance. In order to maintain a driving frequency that is always matched to the device resonant frequency, a positive feedback driving circuit which self-centers the resonance frequency of the membrane has been implemented. The circuitry comprises a pick-up coil, an operational amplifier, and a power field-effect transistor (FET) to drive the excitation coil. The self-centering resonance circuitry has been realized with surface-mount components on a custom printed wiring board suitable for incorporation into the microjet cooler package.

III. Device Characterization

The fabricated microjet cooling device has been characterized in terms of vibration of the membrane and the jet velocity.

The vibration amplitude of the membrane of the microjet cooling device has been measured using a laser interferometer. The laser beam of the vibrometer (spot size approximately 20 μm) was focused on the magnet at the center of the membrane. The output signal of the interferometer (which is proportional to the vibration velocity of the membrane surface) was monitored using a Hewlett-Packard 4195A network/spectrum analyzer. The coil was driven by the same spectrum analyzer. By assuming harmonic vibrations, the vibration amplitude $A = \nu_{\text{surface}}/\omega$ was calculated from the measured surface velocity ν_{surface} and the driving frequency $\omega = 2\pi f$. Fig. 3 shows the vibration amplitude, A, at the center of the membrane for the microjet cooling device as a function of the driving frequency for a driving voltage of $V_{ac} = 450$ mV. Testing of both loaded (with an orifice plate and an orifice diameter of 2.38 mm) and unloaded (without an orifice plate) microjets was performed. The highly nonlinear characteristic

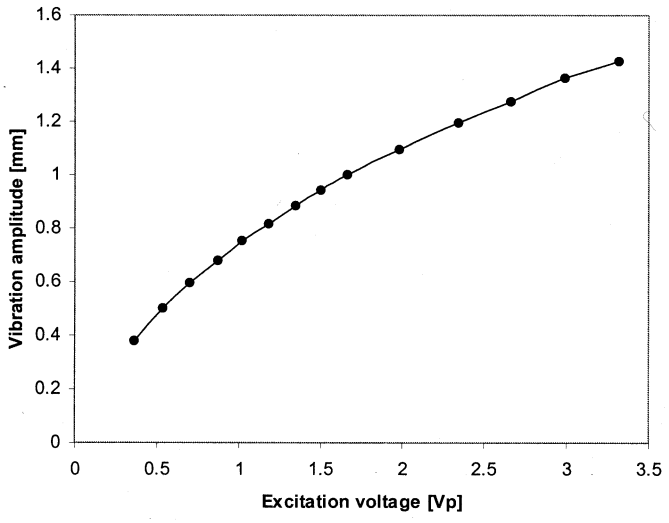

Fig. 4. Vibration amplitude as a function of the excitation voltage at a resonance frequency of 75 Hz.

of the unloaded microjet is likely due to the stress-stiffening effect for large vibration amplitude. This nonlinear effect does not appear in the loaded microjet since the vibration amplitude of the latex membrane is smaller. These lower vibration amplitudes result from the additional damping of the air cavity between the latex membrane and the orifice plate. Fig. 4 shows the vibration amplitude, A, at the center of the membrane as a function of the coil excitation voltage at a frequency of 75 Hz. The vibration amplitude increases with the excitation voltage, as expected.

The average velocity of the synthetic jet emitted from the cooling device has been measured using a miniature total pressure tube which extracts the average velocity of the jet from the pressure difference, ΔP, between the stagnation pressure, P, within the jet and the local static pressure, P_o. The average jet velocity is therefore given by

$$u = \sqrt{\frac{2\Delta P}{\rho}} \tag{1}$$

where ρ is the density of the fluid (in this case, air). Fig. 5 shows the center stream jet velocity of the synthetic jet emitted from the cooling device (orifice of 2.38 mm diameter) as a function of frequency. The velocity measurement was performed by placing the total pressure tube at a distance of 2 mm from the orifice. The total pressure tube was a hypodermic needle with an outer diameter of approximately 0.5 mm and therefore results is some spatial averaging of jet velocity. Because of the induced reversed flow during part of the actuation cycle, the measured centerline velocity within a few jet diameters represents a lower bound for the true velocity (the magnitude of the reversed velocity diminishes rapidly with downstream distance). A maximum jet velocity of approximately 26 m/s was found at a resonance frequency of 99 Hz and a maximum driving power of approximately 1 W. The velocity of the synthetic jet decreases strongly at off-resonance frequencies, as expected from the diaphragm vibration amplitude measurements.

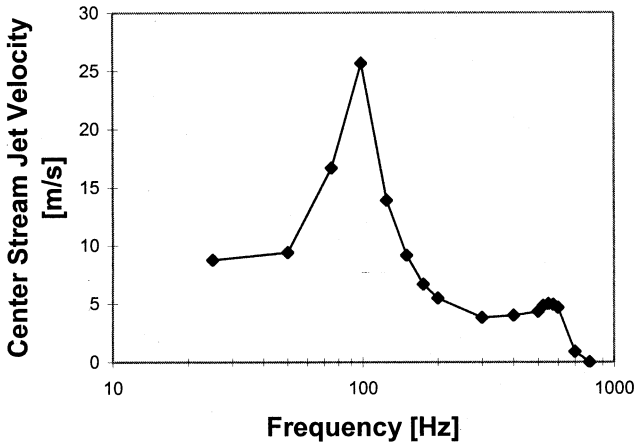

Fig. 5. Center stream jet velocity of the latex membrane microjet as a function of frequency; measurement performed at 2 mm spacing from the orifice.

IV. Cooling Performance Characterization

The cooling performance tests for the microjet cooling devices were accomplished using a 6.4 × 6.4 mm thermal test die (*PST-4, Delco Electronics*) which was mounted in a standard ceramic dual-inline package (*DIP-28*) using conductive silver adhesive. The thermal test die consists of a diode-bridge temperature sensor and a resistive heating element. The heating element was used to heat the die to a certain temperature above ambient for testing purposes. At a constant current, the voltage across a forward-biased diode is proportional to the temperature. The voltage across the bridge was measured using a multimeter connected to a computer. The microjet cooling device was positioned above the thermal test die so that the synthetic jet impinged normal to the surface of the thermal test die, thereby removing heat by forced air convection.

The performance of the microjet cooling devices was measured using the relative reduction (*R.T.R*) of the junction temperature of the thermal test die. The thermal test die was heated by applying up to 9 V (heating power of 1.96 W) to the heating resistor, resulting in an uncooled (free convection) maximum die temperature of 130 °C. The relative temperature reduction due to the heat removal by the impinging synthetic jet is given by

$$R.T.R. = \frac{T_{\text{free}} - T_{\text{jet}}}{T_{\text{free}} - T_{\text{amb}}} \tag{2}$$

where T_{free} is temperature of the die in the case of free convection, T_{jet} is that in the case of forced air convection by jet impingement, and T_{amb} is ambient temperature. The ambient temperature was measured using a digital thermometer and it was located far away from the test setup and any heat sources. A phenomenological study of the microjet cooler with regards to orifice diameter, distance between the cooler and the test die, operation frequency, and driving power, was undertaken.

A. Cooler to Thermal Test Die Spacing

The performance of the microjet cooling device is highly dependent on the spacing (z) between the orifice and the thermal test die. Fig. 6 shows the cooling performance as a function of the orifice to thermal test die spacing. The maximum cooling

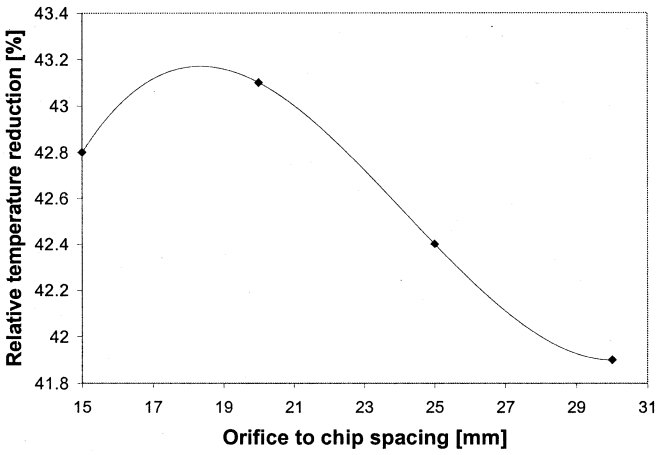

Fig. 6. Cooling performance of the microjet cooling device as a function of spacing from the DIP-28 package (PST-4 thermal test die) to the or fice. Parameters for microjet cooling device are orqice diameter of 2.38 mm, resonance frequency of 80 Hz, and driving power of 0.35 W.

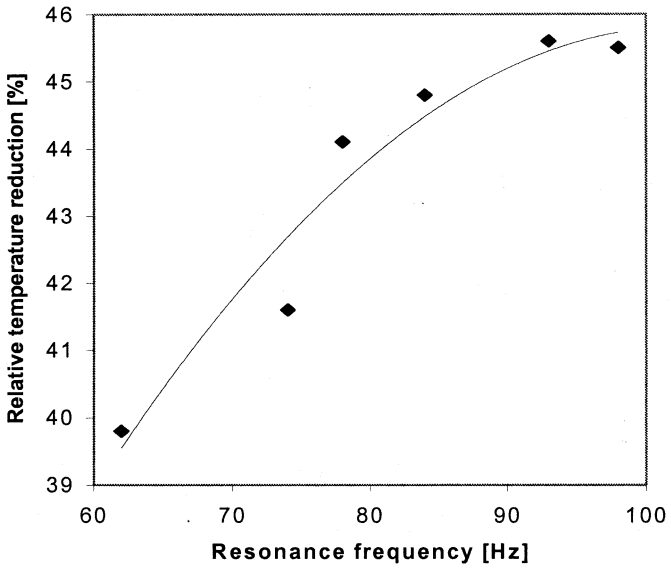

Fig. 7. Cooling performance of the microjet cooling device as a function of resonance frequency. Parameters for microjet cooling device are orifice diameter of $3/32''$, or fice to test die spacing of 15 mm, and driving power of 0.55 W.

performance is achieved when the jet is positioned at approximately 15–20 mm from the surface of the chip $(z/d = 6.3\text{–}8.4)$. For spacing smaller than 15 mm $(z/d < 6.3)$, the cooling performance degrades since the hot air between the orifice plate and the thermal test die is recirculated rather than exchanged with cooler ambient air. This effect has been confirmed by smoke visualization experiments. For spacing larger than 20 mm $(z/d > 8.4)$, the cooling performance decreases due to the decreasing jet velocity.

B. Membrane Resonance Frequency

The amount of air which is moved by the jet over a given time period is proportional to the product of the vibration amplitude and the frequency of the membrane. As seen in Fig. 3, the displacement of the membrane at resonance is approximately three times its off-resonance value. This indicates that maximum air can be moved by increasing the resonant frequency of the membrane. However, this also increases driving power requirements. In order to determine if there is an optimum for membrane resonance frequency, a parametric study was carried out. In order to test cooling performance of the microjet cooling device as a function of the resonance frequency, the mass of the system has been kept constant and the tension of the membrane has been varied. The result is shown in Fig. 7, in which the performance of the microjet cooling device increases as the resonance frequency increases. A predicted maximum in cooling performance for constant driving power could not be achieved due to the material properties of the latex membrane.

C. Orifice Diameter

In order to test cooling performance as a function of orifice diameter, three different orifice plates with different orifice diameters (1.98 mm, 2.38 mm, and 2.78 mm) were utilized. The result (Fig. 8) demonstrates that the performance of the microjet cooling device with the 1.98 mm $(5/64'')$ orifice is low, perhaps due to the increased pressure drop through this smaller orifice. The performance of the 2.78 mm $(7/64'')$ orifice drops off faster

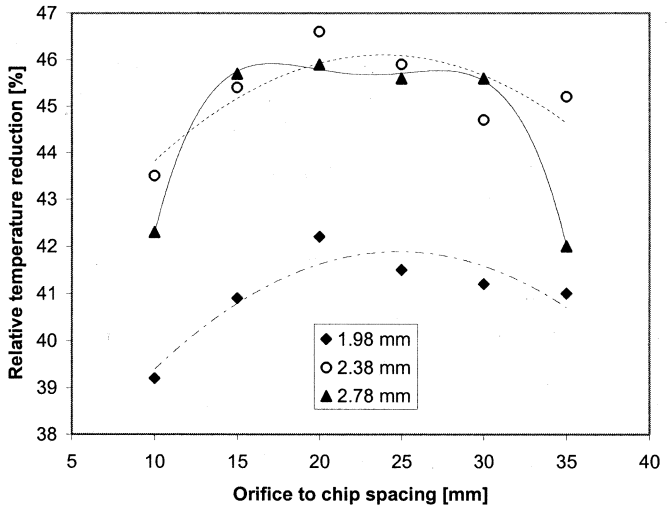

Fig. 8. Cooling performance as a function of the orifice to chip spacing with a variation of the orifice diameters. Driving power and resonance frequency held constant.

at large distances, presumably due to its slower jet velocity. The 2.38 mm $(3/32'')$ orifice shows the best results.

D. Driving Power

The microjet cooling device was positioned at a spacing of 15 mm, with a 2.38 mm orifice diameter and a resonance frequency of 99 Hz. As expected, the cooling performance of the microjet cooling device increases with increasing driving power (Fig. 9). However, the performance begins to saturate at higher driving powers.

V. Dimensionless Analysis of Performance

In order to understand the cooling performance of microjet coolers, a dimensionless analysis of the above results is undertaken. The approach is to use jet-based correlations to obtain

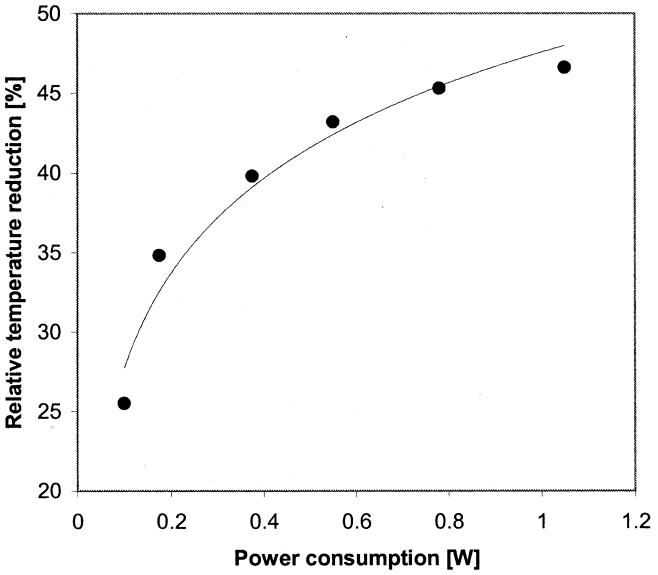

Fig. 9. Cooling performance of a microjet cooling device as a function of power consumption ranging from 0.1 W to 1.1 W.

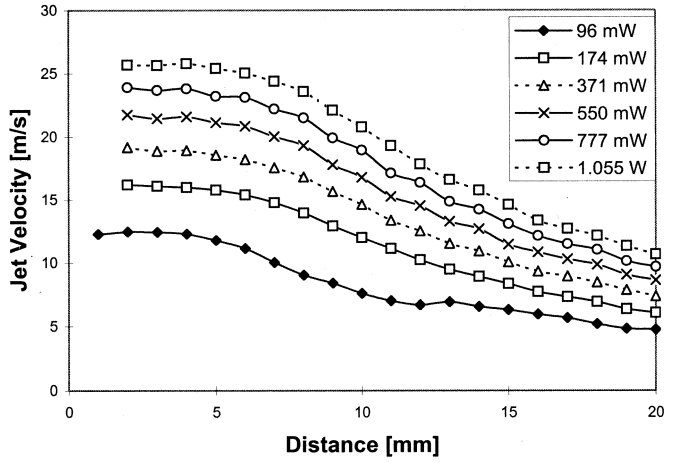

Fig. 10. Center stream jet velocity of the microjet cooling device as a function of the separation distance from the orifice with a variation of the driving power at a fixed resonance frequency.

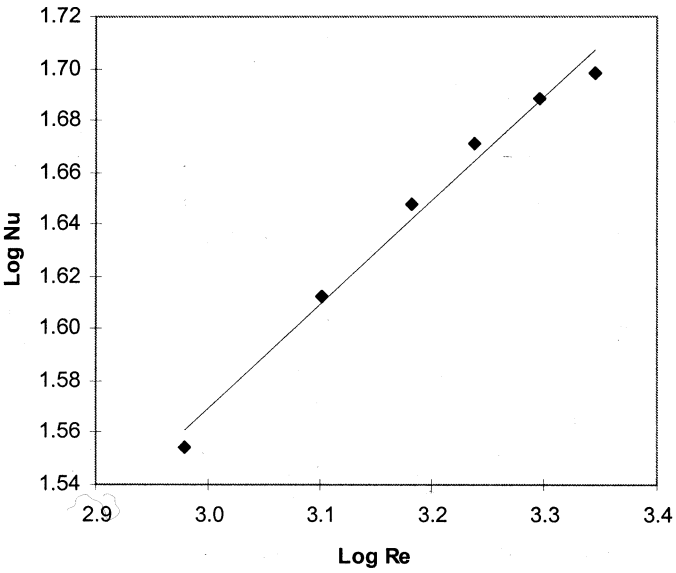

Fig. 11. Heat transfer characteristics at the stagnation point at $z/d = 6.3$ for the microjet cooling device.

the appropriate functional forms of the parameter relations, and extract fitting parameters to match the functional forms to the obtained data. Since there are no reports on synthetic-jet-based heat transfer correlations, previous studies on the heat transfer characteristics of conventional impinging jets [2]–[4], [7] were employed. Due to the difference between the synthetic jet and conventional impinging jet, this discussion only provides qualitative comparison.

In the simplest form, the Nusselt number (Nu) for single circular jet impingement can be expressed by [2]

$$Nu = f\left(\mathrm{Re}, \mathrm{Pr}, \frac{z}{d}, \frac{r}{d}\right) \tag{3}$$

where *Re* is the Reynolds number, *Pr* is the Prandtl number, r is the radial distance from the center of the jet-stagnation point. The turbulence characteristics and the jet velocity (u) depend significantly on the spacing (z/d) from the jet exit plane to the flat heated surface. The optimum spacing (z/d) for the maximum heat transfer at the stagnation point has been reported by Gordon and Carbonpue [7] as $z/d = 6$. The optimum spacings in the microjet cooler are similar to the Gordon and Carbonpue's work [7] and they are in the range of $z/d = 6.3$–8.4 as shown in Fig. 6. Heat transfer coefficients improve with increasing Reynolds number; this relationship can be described as [2]

$$Nu \propto Re^{a} \tag{4}$$

where the characteristic exponent $\mathrm{a} = f(r/d, z/d)$ is typically in the range from 0.5 to 0.8 for conventional jets.

From the jet velocity measurement (Fig. 10) and the cooling performance measurement (Fig. 9) as a function of driving power, the relationship between the Nusselt number and the Reynolds number for the microjet cooling device can be calculated. The results of these calculation are shown in Fig. 11, a log-log plot of the Nusselt number as a function of the Reynolds number. Over the relatively limited range of Reynolds numbers achievable in these experiments, (4) is obeyed. From Fig. 11, the characteristic exponent (a) for the synthetic microjet cooling device is approximately 0.2. This exponent is significantly lower than that obtained for conventional jets. Since these experiments were over a limited range of *Re* and therefore further generalization of the results should be undertaken with some caution [8].

VI. Fan/Jet Cooling Performance Comparison

A standard testbed was used to carry out cooling performance benchmark tests for microjet coolers, CPU cooling fans, and fan/sink combinations. Because larger area chips are more representative of future electronic cooling scenarios, the thermal test die described in Sections II–V were not used. Instead, the testbed design consisted of a larger area resistive heating element and a thermocouple mounted on that element. This assembly was mounted on top of thermally insulating

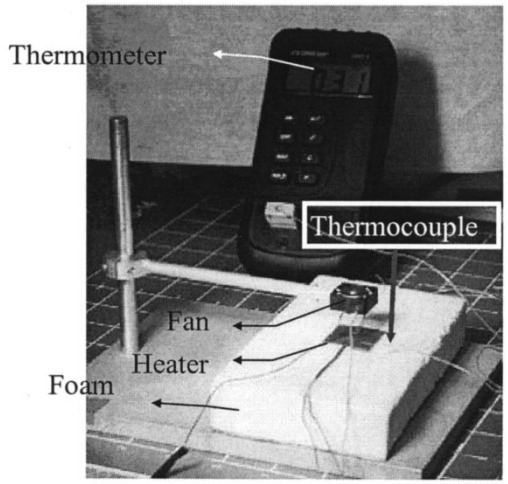

Fig. 12. Photograph of test setup for fan/jet cooling performance comparison.

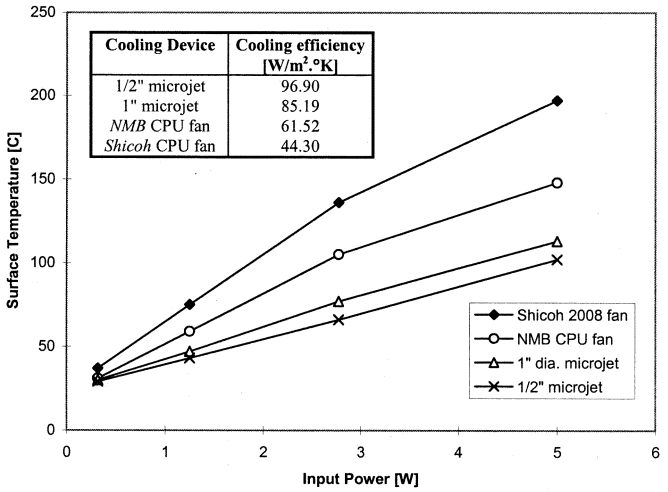

Fig. 13. Surface temperature versus input power of the 1″ square resistive heater for the various cooling devices. The cooling efficiency is defined as the inverse of the slope of the respective data, divided by the heater area.

TABLE I
SPECIFICATIONS OF THE CPU COOLING FANS

	NMB 1606KL-04W-B50	*Shicoh 2008-5*	*Lasagna Cooler*	*Ultra Cooler*
Power	1.02 W	380 mW	110 mW	605 mW
Size L*B*H [mm^3]	40*40*15	20*20*8	50*50*10	57*57*30
Bearing surface	Ball bearing	Brass bushing	Ball bearing	Ball bearing
Airflow [CFM]	*	0.7	8	9.2

foam, thereby minimizing parasitic thermal conduction paths (Fig. 12). Commercially available square Kapton heaters, 25 mm on a side and 50 mm on a side, were used as heat sources. During the cooling tests, the power dissipated by the test heater as well as the temperature of the heater were recorded.

Four different cooling fans were compared to the microjet coolers. Each of these fans is commercially available. The *Shicoh* subminiature fan and the *Lasagna Cooler* are both sold as cooling devices for laptop computers. The *NMB* fan and the *Ultra Cooler* are typical cooling elements for desktop computers. The *Ultra Cooler* has been sold in conjunction with a heat sink designed to clip onto an *Intel Pentium* processor. In some tests, the fan has been removed from this heat sink. The *Lasagna Cooler* is built such that the body of the fan is a heat sink. It should be noted that the heat sink could not be removed in this case. Table I shows a comparison of the specifications of each fan.

The first cooling performance tests were performed using the 25 mm^2 heater. For these tests, two microjets (with diaphragms of 12.5 mm and 25 mm diameter) and two commercially available fans (*NMB* CPU fan and *Shicoh 2008-5*) were tested. The microjets were driven at resonance using a function generator, and the fans driven with a dc power supply.

The microjets and fans were positioned above the test heaters. The separation distance between the jet, or fan, and the heater ranged from 5 mm to 30 mm in steps of 5 mm. After measuring the cooling performance for these distances, an optimum distance for cooling was determined and recorded. In the case of the fans, which have a hub at their center, different lateral positions were also tried to find the best cooling performance, while maintaining a constant vertical position. When the fan hub was positioned off-center, such that the fan blades were positioned over the temperature monitoring point, an approximately 10% cooling performance improvement was noted.

After the ideal position was determined for each of the cooling devices, the comparison tests were performed. The driving powers for the *NMB* CPU fan and the *Shicoh 2008-5* fan are shown in Table I. The driving power for 12.5 mm and 25 mm diameter microjet cooling devices was approximately 200 mW. The resonance frequency of the 25 mm microjet cooling device was approximately 97 Hz and that of the 12.5 mm device was near 105 Hz. The measurement consisted of turning on the cooling, applying various powers to the heating element, waiting for steady state, and recording the temperature resulting from the respective heating power.

The cooling performance benchmark test results are shown in Fig. 13. The graph shows the temperature of the surface of the test heater as a function of the power dissipated by the heater, as parameterized by type of cooling. The slope of the graph is proportional to the thermal resistance. Therefore the lower the slope the better the cooling performance. In this cooling performance benchmark test, it is concluded that microjets (25 mm and 12.5 mm in diameters) outperform both the *NMB* CPU fan and *Shicoh 2008-5* small fan.

The large area heater characterization (50×50 mm^2) was performed using a different set of coolers. A larger microjet (50 mm diameter membrane) was compared to two different cooling fans (*Ultra Cooler* and *Lasagna Cooler*, both of which measure approximately 50 mm on a side). The previously-described test setup was used for the larger heaters.

Microjets and fans were placed on top of the test heater with a separation distance ranging from 5 mm to 40 mm. The *Ultra Cooler* was tested in three different modes: fan only, heat sink only, and fan/sink combination. The *Lasagna Cooler* was tested in two different modes: heat sink only and fan/sink combination. The microjet was tested with three different orifice plates (single orifice, nine orifices, and 13 orifices). The driving power for *Ultra Cooler* CPU fan and *Lasagna Cooler* CPU fan is shown in Table II and the driving power for 50 mm diameter microjet

TABLE II
COMPARISON OF HEAT TRANSFER COEFFICIENTS FOR EACH COOLING DEIVCE ON 2″ SQUARE HEATER COOLING TEST

Cooling Device	Heat Transfer Coefficients [W/m^2.°K]
Ultra Cooler fan/sink	411.16
2" jet / 1 orifice	93.45
Lasagna Cooler fan/sink	85.65
2" jet / 13 orifices	79.07
2" jet / 9 orifices	76.14
Ultra Cooler sink	46.72
Ultra Cooler fan	44.69
Lasagna Cooler sink	24.19

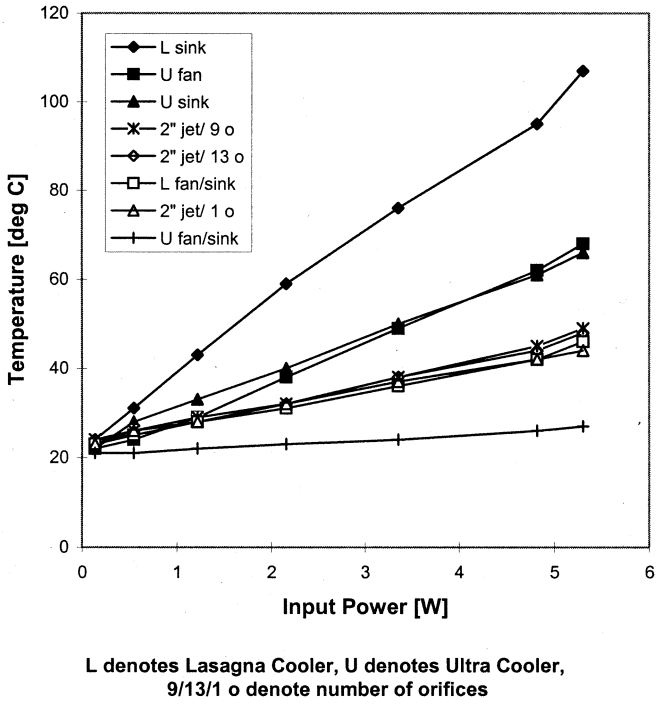

Fig. 14. Surface temperature versus input power of the 2″ square resistive heater for the various cooling devices.

cooling devices was approximately 680 mW. The resonance frequency of the single orifice microjet cooling device was approximately 90 Hz and those of the nine and 13 orifices were 71 Hz and 69 Hz, respectively. Whenever heat sinks were attached to the surface of the heater, silicone thermal conduction compound was applied to the interface between heat sink and the resistive heater to enhance the thermal conduction at the interface. The cooling performance benchmark test results are shown in Fig. 14. In this particular graph, the *Ultra Cooler* fan only mode test was carried out with a separation distance of 15 mm, for 50 mm diameter microjets with a separation distance of 20–30 mm. In these tests the 50 mm diameter microjet outperforms both the *Ultra Cooler*, in heat sink only mode and in fan only mode. The cooling performance of 50 mm diameter microjet is comparable to that of the *Lasagna Cooler* fan/sink. However, the best cooling performance was obtained from the *Ultra Cooler* fan/sink combination.

The sound pressure level measurement setup has been made using sound absorbing acoustical foam as sound insulation wall and WM-034CY195 electret condenser microphone (Panasonic). A preliminary sound pressure level measurement has been carried out using oscilloscope for a 50 mm diameter microjet and *Ultra Coller*. Device under test has been placed directly underneath the microphone with a separation distance of 25 mm. The sound pressure level output from the 50 mm microjet is approximately 0.8 V_{pp} at near resonance frequency, while that of the Ultra cooling fan is approximately 0.1 V_{pp} at near 500 Hz. The microphone we have used in this test has a relatively flat frequency response in the interested frequency range (40 Hz–1 kHz).

VII. CONCLUSION

In this work, microjet cooling devices based on synthetic jet technology have been investigated with respect to thermal management of microelectronic devices. Extensive parameter-based testing of the microjet cooling devices indicates that they can be described by conventional jet correlations with appropriate modification of the correlation parameters. The performance of the microjet coolers is comparable to that of commercially available electronic cooling fans. Microjet-based cooling devices may be especially attractive in localized cooling scenarios since they can be directed onto "hot-spots" in the system.

ACKNOWLEDGMENT

The authors would like to thank Dr. R. Bohlander, Georgia Tech, and P. Black, AMSAM, for valuable technical discussions during the course of this project.

REFERENCES

[1] L. Yeh, "Review of heat transfer technologies in electronic equipment," *J. Electron. Packag.*, vol. 117, Dec. 1995.
[2] K. Jambunathan, E. Lai, M. Moss, and B. Button, "A review of heat transfer data for single circular jet impingement," *Int. J. Heat Fluid Flow*, vol. 13, pp. 106–115, 1992.
[3] D. Zumbrunnen and M. Aziz, "Convective heat transfer enhancement due to intermittency in an impinging jet," *Trans. ASME. J. Heat Transfer*, vol. 115, no. 1, pp. 91–98, Feb. 1993.
[4] H. Sheriff and D. Zumbrunnen, "Effect of flow pulsations on the cooling effectiveness of an impinging jet," *Trans. ASME. J. Heat Transfer*, vol. 116, no. 4, pp. 886–895, Nov. 1994.
[5] R. James, J. Jacobs, and A. Glezer, "A round turbulent jet produced by an oscillating diaphragm," *Phys. Fluids*, vol. 8, no. 9, pp. 2484–2495, Sept. 1996.
[6] D. Coe, M. Allen, M. Trautman, and A. Glezer, "Micromachined jets for manipulation of macro flows," in *Proc. Solid-State Sens. Actuators Workshop*, Hilton Head, SC, 1994, pp. 243–247.
[7] R. Gordon and J. Carbonpue, "Heat transfer between a flat plate and jets of air impinging on it," in *Proc. Int. Develop. Heat Transfer, Int. Heat Transfer Conf.*, Denver, CO, 1962, pp. 454–460.
[8] F. Incropera and D. DeWitt, *Fundamentals of Heat and Mass Transfer*. New York: Wiley, 1985.

Dan S. Kercher received the B.S. and M.S. degrees in physics from the Georgia Institute of Technology, Atlanta, in 1996 and 1998, respectively, where he is currently pursuing the Ph.D. degree in electrical engineering.

During this time, he focused his research on microjet technology and its application to electronics cooling and fluid flow control. After graduation, he worked for IBM Almaden Research Labs as a Research Engineer developing microsystems for hard drive applications. His present research interest is in the creation of nano-structures using MEMS technology.

Jeong-Bong Lee received the B.S. degree in electronics engineering from Hanyang University, Seoul, Korea, in 1986 and the M.S. and the Ph.D. degrees in electrical engineering from the Georgia Institute of Technology (Georgia Tech), Atlanta, in 1993 and 1997, respectively.

He had worked for Georgia Tech as a Research Engineer upon his graduation. In January 1999, he joined Louisiana State University, Baton Rouge, as an Assistant Professor. Since May 2001, he has been with the University of Texas at Dallas, Richardson, as an Assistant Professor in the Department of Electrical Engineering. His current research interests are in the areas of RF/microwave MEMS, MEMS packaging technique, nano-photonic devices, micro/nano assemblers, and chemical/biological sensors.

Dr. Lee received the National Science Foundation's Faculty Early Career Development Award.

Oliver Brand received the M.S. degree in physics from the Technical University Karlsruhe, Germany, in 1990 and the Ph.D. degree from ETH Zurich, Switzerland, in 1994.

From 1995 to 1997, he was a Postdoctoral Fellow at the Georgia Institute of Technology (Georgia Tech), Atlanta. From 1997 to 2002, he worked at the Physical Electronics Laboratory (PEL), ETH Zurich, Zurich, Switzerland, as Lecturer and Group Leader. In January 2003, he joined the Electrical and Computer Engineering Faculty, Georgia Tech. His expertise is in the areas of CMOS-based microsystems, MEMS fabrication technologies, and microsystem packaging.

Mark G. Allen (M'89) received the B.A. degree in chemistry, the B.S.E. degree in chemical engineering, and the B.S.E. degree in electrical engineering from the University of Pennsylvania, University Park, and the S.M. and Ph.D. degrees from the Massachusetts Institute of Technology, Cambridge, in 1989.

He joined the faculty of the Georgia Institute of Technology, Atlanta, in 1989, where he currently holds the rank of Professor and the J. M. Pettit Professorship in Microelectronics. He is North American Editor of the *Journal of Micromechanics and Microengineering*. His research interests are in the areas of micromachining and microelectromechanical systems (MEMS); in particular, the development and application of new fabrication technologies for micromachined devices and systems.

Dr. Allen was General Co-Chair of the 1996 IEEE MEMS Conference.

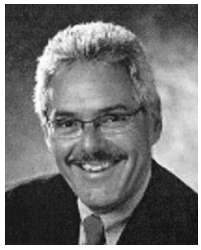

Ari Glezer received the B.S. degree from Tel Aviv University, Israel, in 1974 and the M.S. and Ph.D. degrees from the California Institute of Technology, Pasadena, in 1975 and 1981, respectively.

Prior to joining the faculty of the Georgia Institute of Technology (Georgia Tech), he was a faculty of the University of Arizona. He joined Georgia Tech in 1992, where he currently holds the rank of Professor and the George W. Woodruff Chair in Thermal Systems. His research interests focus on the manipulation and control of shear flows in a broad range of applications, including reacting and nonreacting mixing processes, enhancement of the aerodynamic performance of airborne and underwater vehicles, small-scale combustion-driven power systems, jet thrust vectoring and noise reduction, fluidic-driven heat transfer with an emphasis on electronic cooling, fluid atomization, and the development of novel fluidic actuator technologies including microelectromechanical systems based (MEMS) actuators.